Since January 2020 Elsevier has created a COVID-19 resource centre with free information in English and Mandarin on the novel coronavirus COVID-19. The COVID-19 resource centre is hosted on Elsevier Connect, the company's public news and information website.

Immunobiology 227 (2022) 152192

Contents lists available at ScienceDirect

Immunobiology

journal homepage: www.elsevier.com/locate/imbio

Innate antiviral responses in porcine nasal mucosal explants inoculated with influenza A virus are comparable with responses in respiratory tissues after viral infection

Sofie M.R. Starbæk [a,1], Malene Rask Andersen [b,1], Louise Brogaard [a,2], Anna Spinelli [a], Victoria Rapson [a], Helena Aagaard Glud [a], Lars E. Larsen [c], Peter M.H. Heegaard [a,d], Hans Nauwynck [e], Kerstin Skovgaard [a,*]

[a] Department of Biotechnology and Biomedicine, Technical University of Denmark, Kgs. Lyngby, Denmark
[b] National Veterinary Institute, Technical University of Denmark, Kgs. Lyngby, Denmark
[c] Department of Veterinary and Animal Sciences, University of Copenhagen, Frederiksberg, Denmark
[d] Department of Health Technology, Technical University of Denmark, Kgs. Lyngby, Denmark
[e] Faculty of Veterinary Medicine, Ghent University, Belgium

ARTICLE INFO

Keywords:
Ex vivo
Gene expression
Influenza A virus
Innate immune response
Porcine mucosal explant
Pig
Influenza infection model

ABSTRACT

Nasal mucosal explant (NEs) cultured at an air–liquid interface mimics *in vivo* conditions more accurately than monolayer cultures of respiratory cell lines or primary cells cultured in flat-bottom microtiter wells. NEs might be relevant for studies of host-pathogen interactions and antiviral immune responses after infection with respiratory viruses, including influenza and corona viruses.

Pigs are natural hosts for swine influenza A virus (IAV) but are also susceptible to IAV from humans, emphasizing the relevance of porcine NEs in the study of IAV infection. Therefore, we performed fundamental characterization and study of innate antiviral responses in porcine NEs using microfluidic high-throughput quantitative real-time PCR (qPCR) to generate expression profiles of host genes involved in inflammation, apoptosis, and antiviral immune responses in mock inoculated and IAV infected porcine NEs.

Handling and culturing of the explants *ex vivo* had a significant impact on gene expression compared to freshly harvested tissue. Upregulation (2–43 fold) of genes involved in inflammation, including *IL1A* and *IL6*, and apoptosis, including *FAS* and *CASP3*, and downregulation of genes involved in viral recognition (MDA5 (*IFIH1*)), interferon response (*IFNA*), and response to virus (*OAS1*, *IFIT1*, *MX1*) was observed. However, by comparing time-matched mock and virus infected NEs, transcription of viral pattern recognition receptors (RIG-I (*DDX58*), MDA5 (*IFIH1*), *TLR3*) and type I and III interferons (*IFNB1*, *IL28B (IFNL3)*) were upregulated 2–16 fold in IAV-infected NEs. Furthermore, several interferon-stimulated genes including *MX1*, *MX2*, *OAS*, *OASL*, *CXCL10*, and *ISG15* was observed to increase 2–26 fold in response to IAV inoculation. NE expression levels of key genes involved in antiviral responses including *IL28B* (*IFNL3*), *CXCL10*, and *OASL* was highly comparable to expression levels found in respiratory tissues including nasal mucosa and lung after infection of pigs with the same influenza virus isolate.

1. Introduction

Influenza A virus (IAV) is a zoonotic respiratory pathogen of global importance in veterinary and human health. Although aquatic birds are the natural reservoir for IAV, other species such as humans and pigs can be hosts. IAV belongs to the *Orthomyxoviridae* family and is a single-stranded, negative-sense RNA virus with a characteristic segmented genome. The surface glycoproteins hemagglutinin (HA) and

* Corresponding author at: Kerstin Skovgaard, Department of Biotechnology and Biomedicine, Technical University of Denmark, Søltofts Plads, Building 224, 2800 Kgs. Lyngby, Denmark.
E-mail address: kesk@dtu.dk (K. Skovgaard).
[1] Shared first authorship.
[2] Current affiliation: Department of Veterinary and Animal Sciences, University of Copenhagen, Frederiksberg, Denmark.

https://doi.org/10.1016/j.imbio.2022.152192
Received 9 August 2021; Received in revised form 15 February 2022; Accepted 19 February 2022
Available online 22 February 2022

neuraminidase (NA) determine the virus subtype (Yoon et al., 2014).

IAV infection in mammals is in general restricted to the respiratory tract. IAV enters the hosts through the nasal cavity, where they encounter the mucosal surface as the first barrier towards infection (Starbæk et al., 2018). Infection of host cells is subsequently mediated through attachment of HA to sialic acid(SA)-coated surface glycoproteins of the respiratory epithelium. The configuration of the SA-linkage is considered a major determinant of IAV host specificity, as avian IAV prefer binding to α2,3-linked SAs, while mammalian IAV generally prefer α2,6-linked SAs (Webster et al., 1992; Byrd-Leotis et al., 2017).

Nasal mucosal explants (NEs) cultured at an air–liquid interface resemble the *in vivo* situation more accurately than cells grown in 2D flasks or culture plates. NEs maintain tissue complexity and cell–cell interactions including apical tight junctions, intermediate junctions, and desmosomes of the nasal mucosa of healthy individuals (Denney and Ho, 2018). Furthermore, porcine NEs are easily acquired from slaughterhouses and have been shown to remain viable and exhibit minimal changes in morphology, ciliary beating, and number of apoptotic cells for up to 72 h of cultivation at an air–liquid interface (Glorieux et al., 2007; Tulinski et al., 2013). Porcine NEs therefore represent a highly relevant viral infection model for studies of host-pathogen interactions and pathogenesis. Importantly, using NEs as a replacement for live animals is in accordance with the 3R principle, seeking to reduce the number of animals included in a given study (Tannenbaum and Bennett, 2015).

NE models to study bacterial and viral infection have been established for humans (Jang et al., 2005; Glorieux et al., 2011; Cantero et al., 2013), pigs (Van Poucke et al., 2010), horses (Vairo et al., 2013), cattle (Niesalla et al., 2009; Steukers et al., 2012), sheep (Mazzetto et al., 2020) and ferrets (Roberts et al., 2011). Porcine NEs are low cost and easily available, and both human and porcine NEs have been used in studies of respiratory viruses (Pol et al., 1991; Jang et al., 2005; Glorieux et al., 2007; Van Poucke et al., 2013; Frydas and Nauwynck, 2016), three-dimensional modelling of virus invasion (Glorieux et al., 2009), elucidation of virulence factors of pandemic influenza (Pena et al., 2012), and for comparative analysis of innate immune responses after infection with SARS-CoV-2 and IAV (Alfi et al., 2021). However, to the best of our knowledge, innate immune factors centrally involved in IAV recognition and control have not been studied in porcine nasal explants before.

The similarity of the anatomy (e.g. epithelial cell distribution) of the upper respiratory system including the nasal cavity of pigs and humans has recently been reviewed by us and others (Rajao and Vincent, 2015; Iwatsuki-horimoto et al., 2017; Starbæk et al., 2018). Distribution and quantities of mucus–producing goblet cells and ciliated epithelial cells are highly similar, as is the distribution of SA-coated viral receptors in nasal cavities of pigs and humans, thus rendering porcine NEs a promising model also for human respiratory infections (Spicer et al., 1983; Wallace et al., 1994; Shinya et al., 2006; Zhang et al., 2009; Trebbien et al., 2011).

The antiviral immune response to IAV infection is initiated by recognition of the viral pathogen by pattern recognition receptors (PRR) of the host cells in the nasal mucosa and along the respiratory tract. PRRs such as RIG-I (*DDX58*), TLR3, and MDA5 (*IFIH1*) will detect viral RNA in the host cell cytoplasm and activate the expression of type I and III interferons (IFNs), which induce the expression of a wide range of antiviral interferon-stimulated genes (ISGs) in infected and neighboring cells (Kato et al., 2006; Pichlmair et al., 2006; Brogaard et al., 2018). The local production of ISGs at the site of infection establishes an antiviral state, where components like MX1, OAS1, OASL, and CXCL10 are important for controlling the IAV replication and production of infectious viral progeny during the first days of disease (Skovgaard et al., 2013; Delgado-Ortega et al., 2014; Kim et al., 2015; Brogaard et al., 2018).

To examine the utility of porcine NEs for the study of host responses to IAV infection, 69 NEs isolated from 11 different pigs were used in this study to analyze the transcriptional response to culturing and to IAV exposure.

2. Materials and methods

2.1. Animals

Data presented in this study originates from three independent trials, comprising 69 NEs collected from 11 different pigs (cross-bred Landrace × Yorkshire × Duroc) (Table 1). Animals were acquired from farms of high health status without prior history of respiratory infections. No IAV-specific antibodies were detected in serum samples from the animals prior to the experiment using a commercial ELISA Kit (IDEXX) following the manufacturer's instructions.

Trial 1: 11 NEs were obtained from each of three 6-weeks old piglets (total no. of explants = 33), provided from a herd located in Holbæk, Denmark. The pigs were treated with broad-spectrum antibiotics (200 mg Alamycin containing oxytetracycline, ScanVet, Fredensborg) daily, from three days before euthanasia. At euthanasia, the animals were anesthetized by intramuscular injection of 0.1 ml/kg Zoletil 50 VET (tiletamine 25 mg/ml, zolazepam 25 mg/ml) and euthanized by intracardiac injection of 20 % sodium pentobarbital (KELA, 150 mg/kg).

Trial 2: 12 NEs were obtained from each of two 6-weeks old piglets at Ghent University (total no. of explants = 24). Animals were obtained, treated, and euthanized as described by Glorieux et al. (2007).

Trial 3: Two NEs from each of six 6-weeks old piglets were included in this study (total no. of explants = 12). These animals originated from the same farm as trial 1. Euthanasia was performed as described in trial 1, but animals were not treated with antibiotics prior to euthanasia.

All work has been carried out in accordance with the EU Directive 2010/63/EU for animal experiments.

Gene expression data from nasal mucosal tissue and lung tissue were included for benchmarking our nasal mucosal explants to respiratory tissue isolated from IAV infected pigs (Brogaard et al., 2018; Starbæk et al. in prep). The same A/swine/Denmark/12687/2003 (H1N2) isolate was used for inoculation in all included studies. Lung samples from cross-bred Large White × German Landrace challenged by aerosol exposure were obtained 72 hpi (infected n = 6 and control n = 5) and nasal mucosal tissue from Göttingen Minipigs inoculated by an

Table 1
Sampling and inoculation of nasal mucosal explants. Trial 1 was conducted at the National Veterinary Institute, Technical University of Denmark and included three 6-weeks old pigs, from each of which 11 nasal mucosal explants (NEs) were isolated. Trial 2 included two 6-weeks old pigs from each of which 12 NEs were isolated. This trial was performed at Ghent University, Belgium. Trial 3 was conducted at the National Veterinary Institute, Denmark and included six 6–week old pigs from each of which two explants were isolated. Hours post inoculation (hpi).

Trial	Number of pigs	Number of NEs	Sampling time (hpi)	Number of NEs/time point	Inoculation
1	3	33 (11/pig)	−20	3	3 mock
			0	3	3 mock
			1	9	3 mock + 6 IAV
			24	9	3 mock + 6 IAV
			48	9	3 mock + 6 IAV
2	2	24 (12/pig)	1	8	4 mock + 4 IAV
			24	8	4 mock + 4 IAV
			48	8	4 mock + 4 IAV
3	6	12 (2/pig)	24	6	6 mock
			48	6	6 mock

intranasal mucosal atomisation device were obtained 4 days post infection (infected n = 7 and control n = 5). Further details have been described in (Brogaard et al., 2018; Starbæk et al. in prep respectively).

2.2. Isolation, culture, inoculation, and sampling of nasal mucosal explants

NEs from all trials were isolated and cultured as described by Glorieux et al. (2007) with minor modifications. Briefly, after euthanasia snouts were sawn off the skull in front of the eyes and stripped of skin and muscle tissue. The snouts were split open and mucosa was stripped from the underlying cartilage in the nasal cavity (septum and conchae) and divided into 0.25 cm^2 squares and placed with the epithelium surface upwards on modified cell strainers (VWR) (trial 1 and 3) or stainless-steel supports (trial 2), dimensioned to support the NEs at an air–liquid interface. At this time point (−20 h post inoculation (hpi)), three NEs (trial 1) were harvested and stored in RNAlater (Qiagen). NEs were supplied with serum-free culture medium from the basal side. The NEs were cultured for approximately 20 h at 37 °C and 5% CO_2, before three NEs (trial 1) were collected (0 hpi), divided into two pieces, one half was stored in RNAlater at −20 °C and the other in PBS at −80 °C. The NEs were inoculated with 0.6 ml virus suspension containing 10^4 (trial 2) and 10^5 (trial 1) $TCID_{50}$ of A/swine/Denmark/12687/2003 (H1N2) or virus-free growth medium (mock) (trial 1, 2, and 3) and incubated for 1 h at 37 °C and 5 % CO_2. After inoculation, the explants were washed three times in pre-heated culture medium (37 °C) and placed at an air–liquid interface in fresh pre-heated culture medium (37 °C) (Fig. 1). The culture medium consisted of 1:1 RPMI (Gibco) and DMEM (Gibco) supplemented by 0.1 μg/ml gentamicin (Gibco) and 100 U/ml penicillin and 0.1 mg/ml streptomycin (Gibco) (trial 1 and 2). In trial 3, the amounts of penicillin and streptomycin was increased to 1000 U/ml and 1 mg/ml respectively, gentamicin was increased to 0.5 mg/ml and finally 5 μg/ml amphotericin B "Fungizone" was added to compensate for the lack of pre-euthanasia antibiotic treatment in these piglets compared to the method described by Glorieux et al. (2007). The virus growth medium varied slightly in trypsin concentration (1 μg/ml trypsin TPCK (Sigma-Aldrich) (trial 1 and 3) vs. 0.4 μl/ml (trial 2)). Furthermore, 1 % BME vitamins were added to medium in trial 1 and 3.

NEs were harvested at 1 hpi, 24 hpi, and 48 hpi, one piece stored in RNAlater at −20 °C and the other in PBS at −80 °C (trial 1 and 3). NEs from trial 2 were preserved in one piece in RNAlater. NEs from trial 3 were not inoculated with IAV and were only used in combination with uninfected NEs from trial 1 to study gene expression as a consequence of the *ex vivo* conditions after mock inoculation. Number of pigs and NEs,

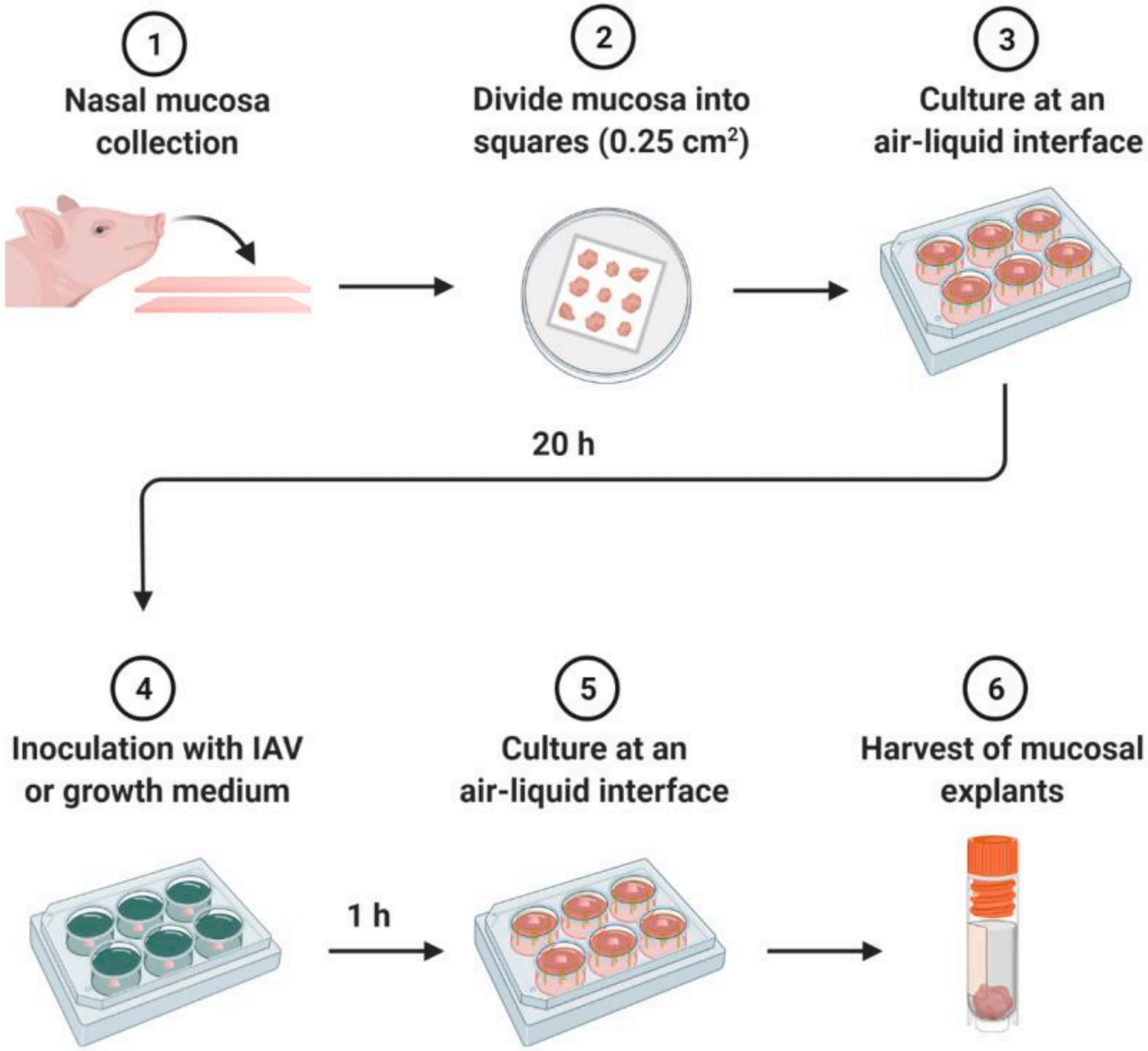

Fig. 1. Schematic representation of the experimental setup. Nasal mucosal isolation (1), air–liquid interface culture procedure (2–3),inoculation with IAV (4), and further cultivation and harvest (5-6). The figure was created with BioRender.com.

as well as treatment and time of harvesting in each trial is summarized in Table 1.

2.3. Viability of cells in nasal mucosal explants and bacterial contamination

The extend of apoptosis was assessed in NEs of trial 2 by termal deoxynucleotidyl transferase dUTP nick end labelling (TUNEL) assay as described by Glorieux et al. (2007). Matrix-assisted laser desorption/ionization time-of-flight mass spectrometry (MALDI-TOF MS) was used to check for bacterial contamination of growth medium before and after NE cultivation as previously described (Nonnemann et al., 2019).

2.4. Reverse transcription (RT)-qPCR analysis

Total RNA was extracted from NEs stabilized in RNAlater as described previously (Barington et al., 2018). Briefly, explants were homogenized in QIAzol Lysis reagent (Qiagen) using gentleMACS M-tubes (Miltenyi Biotec). RNA was extracted using the miRNeasy mini kit (Qiagen) and treated with RNase-free DNase set (Qiagen) according to the manufacturer's instructions. RNA quantity, purity, and integrity were estimated using the Nanodrop ND-1000 spectrophotometer (Saveen and Werner AB) and the Agilent Bioanalyzer (Agilent Technologies), respectively. 500 ng total RNA was used for the cDNA synthesis (QuantiTect Reverse Transcription Kit (Qiagen)) and an additional DNase treatment was included. Two cDNA replicates were prepared for each RNA sample and –RT controls (reverse transcriptase replaced with water) were included in the reverse transcription. Pre-amplification was performed using TaqMan PreAmp Master Mix (Applied Biosystems). A pool of 200 nM qPCR primer mix was prepared by combining primer pairs used in the subsequent qPCR. 5 µl TaqMan PreAmp Master Mix, 2.5 µl 200 nM qPCR primer mix and 2.5 µl cDNA was incubated at 95 °C for 10 min followed by cycles of 95 °C for 15 s and 60 °C for 4 min. Residual primers were digested by adding 16 U of Exonuclease I (New England BioLabs) and incubating at 37 °C for 30 min followed by 80 °C for 15 min.

Microfluidic high-throughput qPCR was performed on a BioMark HD real-time instrument (Fluidigm) as previously described (Brogaard et al., 2018). A number of reference genes were included in the panel of genes to allow normalization of the data. Two different dynamic arrays were used in the present study (GE 96.96 and GE 192.24) combining 96 samples with 96 primer assays and 192 samples with 24 primer assays generating 9216 or 4608 parallel qPCR reactions in a single run, respectively. Primer names, sequences, and length of amplicons used in the present study can be seen in Supplementary Table S1.

After qPCR, data was manually curated using Fluidigm Real-Time PCR Analysis software 3.0.2 (Fluidigm), followed by data pre-processing as previously described (Barington et al., 2018) in GenEx5 (MultiD Analyses AB). GeNorm (Vandesompele et al., 2002) and NormFinder (Andersen et al., 2004) were used to identify the most stable reference genes (using the GenEx5 software). All putative reference genes included (*GAPDH*, *HPRT1*, *RPL13A*, *PPIA*, *YWHAZ*, and *TBP*) were validated as appropriate for normalization and used for data normalization. Relative gene expression levels were calculated after transforming normalized Cq values to relative quantities scaled to the sample in the data set which had the lowest expression of the gene in question. P-values to determine statistical significance of differences in gene expression levels were calculated for mock inoculated explants on LOG2 transformed data using ANOVA, after testing for normal distribution of the data and correcting for multiple testing using Benjamini-Hochberg false discovery rate.

2.5. Virus replication

Tissue culture infectious dose ($TCID_{50}$) was determined as described by Van Poucke et al. (2010) of homogenized NEs, however, the incubation was reduced to three days (trial 1 and 3). Briefly, MDCK cells were inoculated with ten-fold serial dilutions of homogenized NEs collected 24 hpi and 48 hpi and incubated at 37 °C with 5 % CO_2 for three days. Virus replication was confirmed by immunocytochemistry of the MDCK cells, fixed in 99% ethanol and stained using an in-house polyclonal rabbit anti-swine IAV antibody, followed by horse radish peroxidase (HRP) conjugated anti-rabbit immunoglobulins and streptavidin HRP conjugate. The staining was developed by precipitated polymerized ethylcarbazole and inspected using an inverted light microscope. $TCID_{50}$ was calculated by the Reed and Muench approach. For trial 2, viral replication was confirmed by determining $TCID_{50}$ of the NE culture supernatants. MDCK cells seeded in 96-well plates were inoculated in quadruplicate with 10-fold serial dilutions (ranging from 10^0 to 10^{-7}) of NE culture supernatant collected at 24 hpi and 48 hpi, and incubated at 37 °C with 5 % CO_2 for three days. Induction of cytopathic effect (CPE) was recorded and $TCID_{50}$ was calculated by the Reed and Muench approach. Influenza RNA levels in NEs were determined as described above by RT-qPCR targeting the influenza matrix protein gene with the following primers (Nagy et al., 2010); Forward Sequence (5′ to 3′) GGCCCCCTCAAAGCCGA and Reverse Sequence (5′ to 3′) CGTCTACGYTGCAGTCC as well as in-house primers targeting the HA gene. The level of initial viral RNA (average of matrix protein assay and HA assay) from the inoculum was measured at 1 hpi, and was scaled to 1 in order to measure any relative increase from this time point.

3. Results

3.1. Gene expression changes during ex vivo explant culture

Changes in gene expression as a consequence of *ex vivo* culturing were studied for 82 genes involved in inflammation, apoptosis, and antiviral immune responses (Supplementary Table S1) in mock inoculated porcine NEscollected at necropsy (–20 hpi), after 20 h of acclimatization (0 hpi), and at 24 hpi and 48 hpi. Multivariate analysis (principal component analysis (PCA)) of gene expression data, from a total of 24 explants across the four time points, identified three clusters of NE samples having comparable gene expression profiles (Fig. 2, top panel). NEs collected at necropsy (-20 hpi) form one cluster (green), those collected following 20 h of *ex vivo* acclimatization (time 0 hpi) form a second cluster (yellow), while the third cluster is constituted of NE samples collected at both 24 and 48 hpi (red and dark red). Thus, despite of differences in trial 1 and 3, 24 hpi and 48 hpi was clearly separated from earlier time points. RNA quality, shown as RNA integrity numbers (RIN), was not affected by the duration of culturing (Fig. 2, bottom panel).

Quantification of specific mRNA changes resulting from culturing by itself revealed a significant regulation of 24 genes after correction for multiple testing (see Supplementary Table S2). These genes were mainly involved in inflammation or response to inflammation. However, genes involved in apoptosis and response to viral infection were also regulated (see Supplementary Table S2 and Fig. 2, bottom panel). Importantly, several key genes involved in innate antiviral immune response including viral PRRs (MDA5 (*IFIH1*) and *TLR8*), Type I IFNs (*IFNA* and *IFNB1*), and ISGs (*OAS1*, *MX1* and *RNASEL*) were significantly down-regulated 2–10 fold during culturing. Genes involved in inflammatory response such as *IL1A* and *IL6* were on the contrary upregulated 4 to 44 fold (Fig. 2, bottom panel) after culturing. Furthermore, the acute-phase protein serum amyloid A (SAA) was also found to be significantly upregulated at all three time points following culturing.

3.2. Gene expression changes in mucosal explants exposed to influenza A virus during culture

The response to IAV exposure in explants grown at an air liquid interface were analyzed for genes involved in antiviral immune responses and compared to time-matched mock controls. Expression of

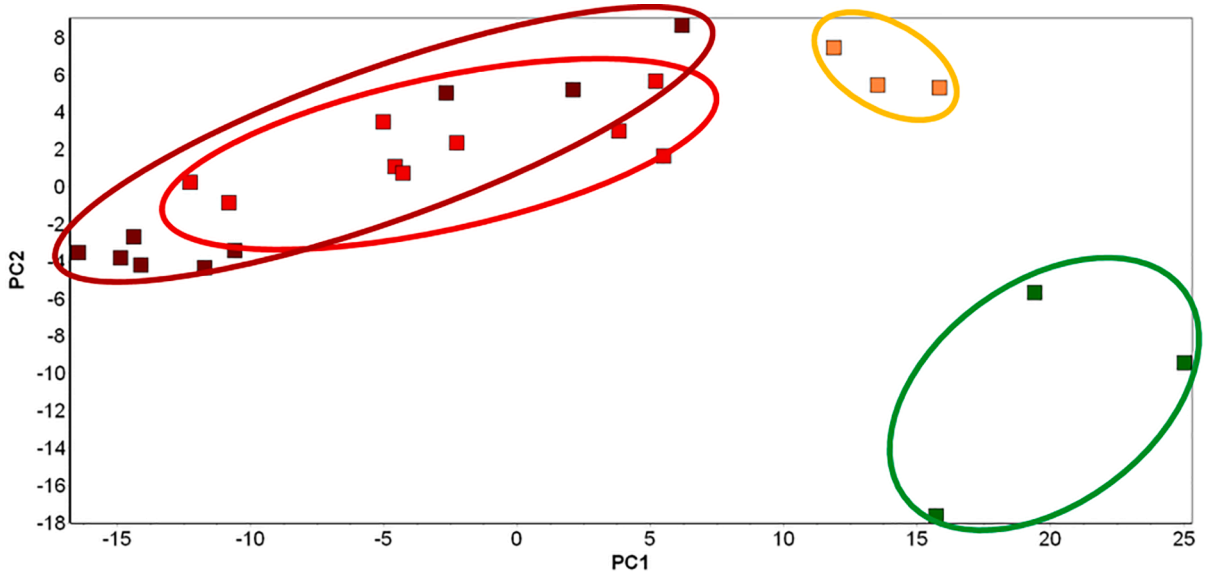

	Genes involved in inflammation					Genes involved in antiviral response				Reference genes			RIN values	Number of mock inoculated animals/explants
	IL1A	*IL6*	*SAA*	*CCL20*	*CXCL2*	*MDA5*	*IFNA*	*IRF7*	*MX1*	*PPIA*	*TBP*	*YWHAZ*		
-20 hours	1.0	1.0	1.0	1.0	1.0	1.0	1.0	1.0	1.0	1.0	1.0	1.0	8.8	3/3
SEM	0.1	0.9	0.5	0.2	0.7	0.2	0.2	0.5	0.4	0.1	0.0	0.1	0.5	
0 hours	9.6	43.5	4.1	8.7	13.4	1.1	0.4	0.5	0.6	1.2	0.8	1.2	8.3	3/3
SEM	1.9	2.2	1.1	1.4	1.7	0.1	0.1	0.2	0.1	0.1	0.1	0.1	0.4	
24 hours	8.8	9.8	4.6	10.2	10.2	0.7	0.2	0.2	0.2	1.2	1.0	1.3	8.6	9/9
SEM	1.0	1.1	0.8	2.2	1.3	0.1	0.0	0.1	0.1	0.1	0.0	0.1	0.2	
48 hours	7.1	10.9	5.5	12.5	4.8	0.5	0.3	0.1	0.2	1.3	1.0	1.2	9.0	9/9
SEM	1.0	4.5	1.7	7.3	0.8	0.1	0.1	0.0	0.1	0.1	0.1	0.1	0.2	
P-value	6.30E-07	4.64E-05	1.18E-02	1.18E-02	5.43E-04	1.15E-02	2.38E-03	9.38E-03	5.00E-04	NS	NS	NS	NS	

Fig. 2. Gene expression analysis of mock inoculated control mucosal explants from trial 1 and 3. Top panel: Principal component analysis (PCA) of gene expression data from 82 genes involved in inflammation and antiviral immune response. Green: Nasal mucosa collected directly from the pig at euthanasia (-20 hpi), Orange: Nasal mucosa explants after 20 h acclimatization in the culture system (0 hpi), Red: Nasal mucosa cultured in virus free medium, sampled 24 hpi, Dark red: Nasal mucosa cultured in virus free medium, sampled 48 hpi. PC = Principal component. Bottom panel: Changes of expression in genes involved in inflammation, antiviral immune response and reference genes. Expression data are scaled to the mean values of −20 hpi explants (scaled to 1). SEM = Standard error of mean; RIN = RNA Integrity Number; NS = not significant. P–values to determine statistical significance of differences in gene expression levels over time were calculated using ANOVA.

several pattern recognition receptors including RIG-I (*DDX58*), MDA5 (*IFIH1*), *TLR3*, and the downstream regulatory factor *IRF7* was upregulated in virus inoculated NEs compared to the mock inoculated NEs at 24 hpi (Fig. 3).

Likewise, the expression of *MX1* and *MX2* was upregulated following IAV inoculation at 24 hpi. Type I IFN (*IFNB1*) and type III IFN (*IL28B* (*IFNL3*)), several ISGs (*ISG15*, *IFITM1*, *IFITM3*, *OAS1*, *OASL*, *EIF2AK2*), and the chemokines *CXCL10* and *CXCL2* were found to be upregulated between 3 and 26 fold in IAV infected NEs at 48 h after viral exposure, compared to mock inoculated NEs harvested at the same time point (Table 2). Increased expression of both IFNs and ISGs from 24 h to 48 h after IAV infection is seen in all investigated antiviral genes compared to

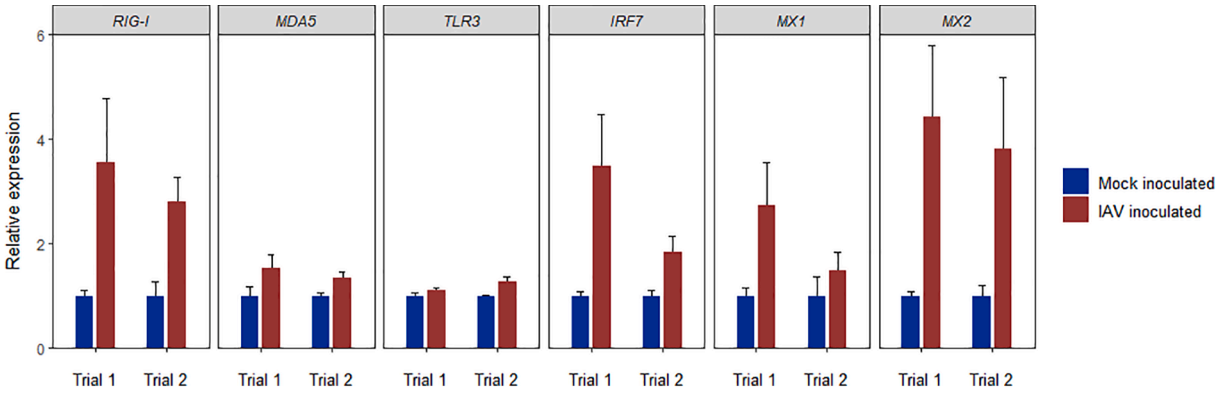

Fig. 3. Relative expression of the pattern recognition receptors RIG-I (*DDX58*), MDA5 (*IFIH1*), *TLR3,* and transcription factor *IRF7* as well as the ISGs *MX1* and *MX2*, 24 h after mock inoculation (blue, scaled to 1) or viral inoculation (red) of porcine NEs. Relative expression is presented as mean relative expression ± SEM. Descriptive statistics were used due to small group size. Trial 1 infected n = 6, control n = 3 and trial 2 infected n = 4, control n = 4.

Table 2
Differential expression of antiviral genes from mock and virus inoculated explants 24 h and 48 h after inoculation (trial 2). Data is presented as mean relative expression ± SEM in brackets. Differentially expression of more than two folds in the NE are shown in bold. Descriptive statistics were used due to small group size.

Gene	Explant mock 24 h	Explant inoculated 24 h	Explant mock 48 h	Explant inoculated 48 h
CCL2	1 (0.1)	1.1 (0.1)	**1 (0.1)**	**2.0 (0.3)**
CXCL10	**1 (0.2)**	**3.9 (1.5)**	**1 (0.2)**	**17.7 (4.8)**
IFNB1	1 (0.1)	1.2 (0.4)	**1 (0.2)**	**3.3 (1.1)**
IL28B (IFNL3)	**1 (0.3)**	**5.4 (3.5)**	**1 (0.2)**	**15.7 (5.4)**
ISG15	**1 (0.2)**	**2.1 (0.5)**	**1 (0.1)**	**9.1 (0.8)**
IFITM1	1 (0.2)	1.2 (0.1)	**1 (0.1)**	**2.7 (0.6)**
IFITM3	1 (0.1)	1.2 (0.2)	**1 (0.1)**	**3.5 (0.6)**
OASL	**1 (0.4)**	**2.0 (0.7)**	**1 (0.3)**	**9.1 (1.5)**
OAS1	**1 (0.1)**	**4.9 (1.6)**	**1 (0.1)**	**25.8 (4.3)**
EIF2AK2	1 (0.2)	1.8 (0.4)	**1 (0.1)**	**4.8 (0.4)**

Table 3
Viral replication determined by infectious dose 50% endpoint (TCID50) in MDCK cells, calculated using Reed and Muench method (Reed and Muench, 1938) and RNA expression measured by RT-qPCR. qPCR data is expressed as mean relative expression ± SEM compared to 1 h post inoculation, nvd = no virus detected.

	Infectious viral titer (TCID50)		Viral RNA (relative quantities)		
Experiment	24 h	48 h	1 h PI	24 h PI	48 h PI
NE trial 1	nvd	nvd	1 (0.2)	2.5 (1.3)	3.4 (2.6)
NE trial 2	5.9 (log10 TCID50/ml)	7.1 (log10 TCID50/ml)	1 (0.5)	146 (137)	487 (127)

their time matched controls (Table 2).

In order to compare changes in expression of antiviral genes in explants of the present study with respiratory tissue from experimentally IAV infected pigs (Brogaard et al., 2018; Starbæk et al. in prep.), selected data of gene expression is illustrated in Fig. 4. Comparable changes in expression of key innate antiviral genes including *IL28B* (*IFNL3*), *OASL*, and *CXCL10* were seen between cultured NEs 24 h after viral exposure and nasal mucosal tissue and lung tissue isolated from pigs three to four days after infection with the same influenza isolate, A/swine/Denmark/12687/2003 (H1N2) (Fig. 4).

Infectious viral titer and viral RNA levels are seen in Table 3. Virus replication could only be detected in trial 2, at 24 and 48 hpi. Viral RNA was detected in infected NEs by qPCR, and increased over time, but at different rates in trial 1 and 2.

Low to moderate levels of apoptotic cells were detected by TUNEL assay. However, no distinct association was found between the extend of apoptotic cells and cultivation time or infection status of the NEs (data not shown). In contrast, several genes associated with apoptosis including *FAS*, *FOS* and *CASP3* were upregulated 2–4 fold at the three time points following −20 hpi. (Table S2). No bacterial contamination was found in the growth medium of explants using MALDI-TOF MS.

4. Discussion

The local innate immune response to infection by IAV is a highly complex process orchestrated by numerous respiratory epithelial cells and epithelium-associated immune cells. The process of viral recognition and activation of signalling pathways leading to type I and III IFN production and subsequent upregulation of antiviral ISGs is paramount for the early control and elimination of any IAV infection (Bowie and Unterholzner, 2008; Starbæk et al., 2018). The epithelium of the nasal mucosa is composed of ciliated cells, secretory cells, and basal cells attached to each other by tight junctions and immune cells, notably resident macrophages and dendritic cells (Knight and Holgate, 2003; Jahnsen et al., 2004; Beule, 2010). This highly multifaceted respiratory environment can be approximated using nasal explants grown at an air–liquid interface for a limited time period (Glorieux et al., 2007; Van Poucke et al., 2010). After isolation, culturing, and inoculation of porcine NEs, we were able to study the molecular antiviral immune response to IAV at the site of infection, in time-matched mock and virus infected explants up to 48 h after viral exposure.

In the present study no decrease in RNA quality or significant correlation of number of apoptotic cells over time was seen in response to *ex vivo* culturing, which is in accordance with previous results obtained with this model, showing no or little apoptosis and necrosis up to 96 h of *ex vivo* culturing (Glorieux et al., 2007; Van Poucke et al., 2010). Not surprisingly, the environmental change from *in vivo* to *ex vivo* resulted in increased expression of several pro-inflammatory genes, such as *IL1A* and *IL6* and genes associated with apoptosis including *FAS* and *CASP3*. In addition, genes involved in viral pathogen recognition, IFN signalling, and several ISGs were found to be regulated over time during cultivation in the absence of virus. Most of these genes were downregulated. These important and opposite effects on the gene expression of pro-inflammatory as opposed to antiviral immune genes solely brought about by the change in environment, strongly highlight the importance of including and standardizing data to time and handling matched mock controls when studying molecular antiviral immune responses to IAV infection in NEs.

Following IAV inoculation, the expression of several PRRs important

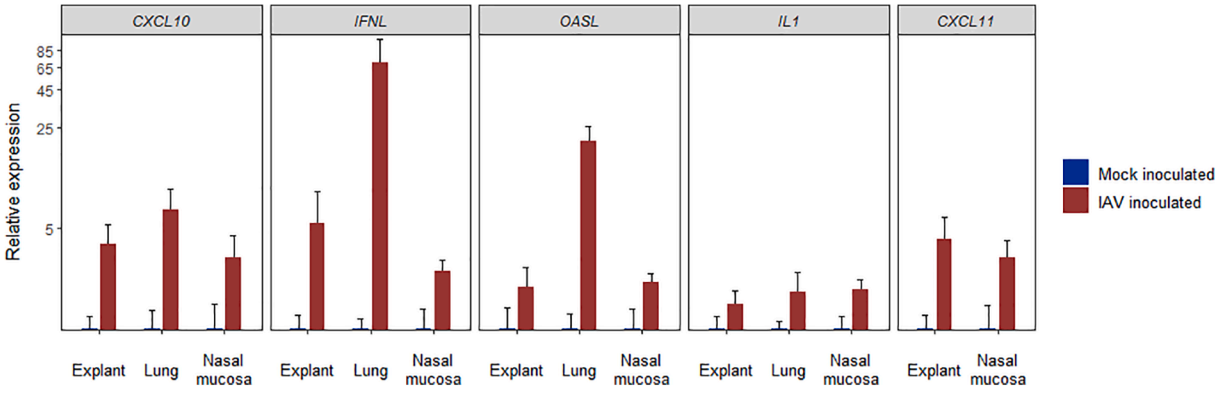

Fig. 4. Comparable expression of key innate antiviral genes within cultured explants at 24 h post inoculation compared with *in vivo* nasal mucosal tissue and lung tissue isolated from pigs infected with the same IAV isolate. Lung data was obtained 3 days post IAV infection (control n = 5 and infected n = 6). Nasal mucosal tissue was collected 4 days post inoculation (control n = 5 and infected n = 7). Relative expression is presented as mean expression ± SEM. Please note the log2 scale on the Y-axis. Descriptive statistics were used due to small group size.

for detection of viral RNA was induced in NEs, including RIG-I (*DDX58*) and MDA5 (*IFIH1*). We have previously studied the innate immune response in lungs of IAV infected pigs inoculated with the same viral isolate used in the present study, A/swine/Denmark/12687/2003 (H1N2) (Skovgaard et al., 2013; Brogaard et al., 2018). Although the change in gene expression depends on cell composition of the tissue and number of infecting virus particles, gene expression patterns in NEs, nasal mucosa, and lung tissue show comparable patterns of expression for selected antiviral genes. The moderate to high upregulation of *IL28B* (*IFNL3*), *OASL*, and *CXCL10* seen in this study was in accordance with previously reported regulation in lung tissue (Brogaard et al., 2018) as well as nasal mucosal tissue isolated from pigs infected with the same IAV isolate (Starbæk et al. in prep.).

A strong but transient IFN response is of great importance during viral infection. In the present study, *IFNB1* was upregulated in IAV infected NEs 48 h after virus exposure compared to mock inoculated NEs harvested at the same time point. Upregulation of *IFNB1* was also found in human nasal epithelial cells 24 h and 48 h after exposure to human H3N2 by Tan et al. (2018). Type III interferon (IFN-λ) has been shown to be among the primary interferons produced by epithelial and dendritic cells in response to IAV infections of the upper respiratory tract (Jewell et al., 2010; Yan et al., 2016; Klinkhammer et al., 2018; Tan et al., 2018). In the present study, *IL28B (IFNL3)* was found to be upregulated in infected NEs at both 24 hpi and 48 hpi. The results of both type I and III IFNs mirrors previously results obtained from *in vivo* infected pig lungs and nasal mucosal tissue with the same viral isolate (Brogaard et al., 2018; Starbæk et al. in prep) as well as in human nasal epithelial cells in response to H3N2 IAV infection (Yan et al., 2016; Tan et al., 2018).

MX1 and *MX2* were upregulated after viral inoculation in both trial 1 and 2. *MX1* is a homolog to the mouse *Mx1* involved in inhibition of viral transcription in the nucleus (Dreiding et al., 1985; Verhelst et al., 2012), whereas the porcine *MX1* is found in the cytoplasm, where it interferes with transport of viral particles to the nucleus, hence inhibiting viral replication (Palm et al., 2010). Upregulation of *MX1* has previously been reported in human nasal epithelial cells infected with H1N1 (Kim et al., 2015) and in human blood samples from individuals infected with influenza virus (Andres-Terre et al., 2015). Upregulation of *MX2* has previously been reported in IAV infected porcine lung explants, both in case of single–infection with a H1N1 swine IAV and co–infection with swine IAV (H1N1) and porcine reproductive and respiratory syndrome virus (PRRSV) (Dobrescu et al., 2014) and after infection with H3N2 swine IAV (Delgado-Ortega et al., 2014). However, the *MX2* gene has to our knowledge, not previously been reported to be involved in response to IAV infection of the upper respiratory system in pigs, and its relevance in porcine nasal mucosal tissue remains to be studied in detail.

Other interferon stimulated genes important for influenza viral restriction early after infection, including *CXCL10*, *OAS1*, *OASL*, and *ISG15*, were found to be highly upregulated in NEs 48 hpi. *CXCL10* has previously been found upregulated in human nasal epithelial cells after infection with human H3N2 (Tan et al., 2018) and *CXCL10* and *OAS1* have been reported to participate in control of infection through suppression of transcription or replication of IAV in human nasal epithelium (Kim et al., 2015). Furthermore, OAS becomes catalytically active in the epithelial cell cytosol upon binding of viral double stranded RNA (dsRNA) during the IAV replication cycle. This activation promotes OAS mediated degradation of viral RNA through RNase L activity and in turn inhibits viral replication (Min and Krug, 2006; Drappier and Michiels, 2015).

Replication of IAV in NEs has previously been reported (Van Poucke et al., 2010). Viral RNA measured by qPCR increased modestly in trial 1 compared to trial 2, and no infectious virus was detected in trial 1. However, reduced viral replication seemed to have only minor effects on the magnitude of antiviral immune responses measured in NEs. Comparing the patterns of gene regulation between trial 1 and 2 for key antiviral genes revealed no systematic differences. Future studies are needed to address the difference in viral replication in order to obtain more reproducible results.

In general, the use of NEs provides easily accessible, cheap samples, and limited space requirements compared to a similar *in vivo* setup with live pigs. However, it of course comes with some limitations; The NEs are removed from the organism and its natural environment. The tissue lacks the lymph system and influx of immune cells and other immune-related components. Future studies should hold more biological replicates in order to allow statistical analysis on all data. Furthermore, the experimental settings should be standardized completely between different trials so pigs and NEs are treated under the same conditions and inoculated with the same amount of virus particles. The lack of antibiotic treatment in trial 3 was compensated by using time-matched controls to adjust for a possible difference in the baseline. The presence of other respiratory viruses was not examined, however, nasal explants were isolated from pigs acquired from farms of high health status without prior history of respiratory infections. Therefore, the presence of other respiratory virus cannot be excluded, but it would reflect a natural environment in the nasal mucosa. Virus enters host cells from the apical side of epithelial cells in the airways. In order to mimic nature more closely, virus could be administered on top of the NEs i.e. from the apical side of the cells instead of immersing NEs into virus suspension. Furthermore, it could be speculated, that the incubation temperature should be decreased a few degrees to mimic the nature of a slightly colder environment of the snout/nose. Finally, the TUNEL assay detects DNA fragmentation, which occurs in the late phase of apoptosis. Assays detecting early stage apoptosis, such as caspase activation assay, should be used in future studies.

High similarity of human and pig respiratory epithelium anatomy and antiviral immune proteins (Dawson et al., 2013; Starbæk et al., 2018) suggests that porcine NEs could be a relevant 3R compliant model for the study of early innate host defence against both swine and human adapted IAV. In conclusion, we have shown that NEs are an important valid method for the study of the innate antiviral immune response after IAV infection, though gene expression changes solely as a consequence of *ex vivo* culturing. However, by careful analysis of time and handling matched mock control samples, transcriptional analysis of the innate antiviral immune response is indeed possible and comparable to responses measured in nasal mucosal tissue and lung tissue isolated from IAV infected pigs.

Funding

The work presented in this article is part of the FluZooMark project supported by Novo Nordisk Foundation (grant NNF19OC0056326).

CRediT authorship contribution statement

Sofie M.R. Starbæk: Conceptualization, Data curation, Formal analysis, Investigation, Methodology, Project administration, Validation, Vizualization, Writing - origional draft, Writing - review & editing. **Malene Rask Andersen:** Data curation, Formal analysis, Investigation, Methodology, Writing – original draft, Writing – review & editing. **Louise Brogaard:** Data curation, Formal analysis, Methodology, Writing – review & editing. **Anna Spinelli:** Formal analysis, Methodology, Writing – review & editing. **Victoria Rapson:** Formal analysis, Methodology, Writing – review & editing. **Helena Aagaard Glud:** Formal analysis, Methodology, Visualization, Writing – review & editing. **Lars E. Larsen:** Funding acquisition, Methodology, Writing – review & editing. **Peter M.H. Heegaard:** Methodology, Writing – review & editing. **Hans Nauwynck:** Methodology, Writing – review & editing. **Kerstin Skovgaard:** Conceptualization, Formal analysis, Funding acquisition, Methodology, Project administration, Supervision, Writing – review & editing.

Declaration of Competing Interest

The authors declare that they have no known competing financial interests or personal relationships that could have appeared to influence the work reported in this paper.

Acknowledgements

We thank Bettina Nonnemann (Department of Health Technology, Technical University of Denmark) for practical support of quality control (MALDI-TOF MS) throughout this study. We also thank Karin Tarp (Department of Biotechnology and Biomedicine, Technical University of Denmark) for technical assistance for performing qPCR.

Appendix A. Supplementary data

Supplementary data to this article can be found online at https://doi.org/10.1016/j.imbio.2022.152192.

References

Alfi, O.r., Yakirevitch, A., Wald, O., Wandel, O., Izhar, U., Oiknine-Djian, E., Nevo, Y., Elgavish, S., Dagan, E., Madgar, O., Feinmesser, G., Pikarsky, E., Bronstein, M., Vorontsov, O., Jonas, W., Ives, J., Walter, J., Zakay-Rones, Z., Oberbaum, M., Panet, A., Wolf, D.G., Heise, M.T., 2021. Human nasal and lung tissues infected ex vivo with SARS-CoV-2 provide insights into differential tissue-specific and virus-specific innate immune responses in the upper and lower respiratory tract. J. Virol. 95 (14).

Andersen, C.L., Jensen, J.L., Ørntoft, T.F., 2004. Normalization of real-time quantitative reverse transcription-PCR data: a model-based variance estimation approach to identify genes suited for normalization, applied to bladder and colon cancer data sets. Cancer Res. 64 (15), 5245–5250. https://doi.org/10.1158/0008-5472.CAN-04-0496.

Andres-Terre, M., McGuire, H., Pouliot, Y., Bongen, E., Sweeney, T., Tato, C., Khatri, P., 2015. Integrated, multi-cohort analysis identifies conserved transcriptional signatures across multiple respiratory viruses. Immunity 43 (6), 1199–1211. https://doi.org/10.1016/j.immuni.2015.11.003.

Barington, K., Skovgaard, K., Henriksen, N.L., Johansen, A.S.B., Jensen, H.E., 2018. The intensity of the inflammatory response in experimental porcine bruises depends on time, anatomical location and sampling site. J. Forensic Leg. Med. 58, 130–139. https://doi.org/10.1016/j.jflm.2018.06.005.

Beule, A.G., 2010. Physiology and pathophysiology of respiratory mucosa of the nose and the paranasal sinuses. GMS Curr. Top. Otorhinolaryngol. – Head Neck Surg. 9, 1–24. https://doi.org/10.3205/cto000071.

Bowie, A.G., Unterholzner, L., 2008. Viral evasion and subversion of pattern-recognition receptor signalling. Nat. Rev. Immunol. 8 (12), 911–922. https://doi.org/10.1038/nri2436.

Brogaard, L., Larsen, L.E., Heegaard, P.M.H., Anthon, C., Gorodkin, J., Dürrwald, R., Skovgaard, K., Renukaradhya, G.J., 2018. IFN-λ and microRNAs are important modulators of the pulmonary innate immune response against influenza A (H1N2) infection in pigs. PLoS ONE 13 (4), e0194765. https://doi.org/10.1371/journal.pone.0194765.

Byrd-Leotis, L., Cummings, R.D., Steinhauer, D.A., 2017. The interplay between the host receptor and influenza virus hemagglutinin and neuraminidase. Int. J. Mol. Sci. 18, 1–22. https://doi.org/10.3390/ijms18071541.

Cantero, D., Cooksley, C., Jardeleza, C., Bassiouni, A., Jones, D., Wormald, P.-J., Vreugde, S., 2013. A human nasal explant model to study Staphylococcus aureus biofilm in vitro. Int. Forum Allergy Rhinol. 3 (7), 556–562. https://doi.org/10.1002/alr.21146.

Dawson, H.D., Loveland, J.E., Pascal, G., Gilbert, J.GR., Uenishi, H., Mann, K.M., Sang, Y., Zhang, J., Carvalho-Silva, D., Hunt, T., Hardy, M., Hu, Z., Zhao, S.-H., Anselmo, A., Shinkai, H., Chen, C., Badaoui, B., Berman, D., Amid, C., Kay, M., Lloyd, D., Snow, C., Morozumi, T., Cheng, R.-Y., Bystrom, M., Kapetanovic, R., Schwartz, J.C., Kataria, R., Astley, M., Fritz, E., Steward, C., Thomas, M., Wilming, L., Toki, D., Archibald, A.L., Bed'Hom, B., Beraldi, D., Huang, T.-H., Ait-Ali, T., Blecha, F., Botti, S., Freeman, T.C., Giuffra, E., Hume, D.A., Lunney, J.K., Murtaugh, M.P., Reecy, J.M., Harrow, J.L., Rogel-Gaillard, C., Tuggle, C.K., 2013. Structural and functional annotation of the porcine immunome. BMC Genomics 14 (1). https://doi.org/10.1186/1471-2164-14-332.

Delgado-Ortega, M., Melo, S., Punyadarsaniya, D., Ramé, C., Olivier, M., Soubieux, D., Marc, D., Simon, G., Herrler, G., Berri, M., Dupont, J., Meurens, F., 2014. Innate immune response to a H3N2 subtype swine influenza virus in newborn porcine trachea cells, alveolar macrophages, and precision-cut lung slices. Vet. Res. 45 (1) https://doi.org/10.1186/1297-9716-45-42.

Denney, L., Ho, L.-P., 2018. The role of respiratory epithelium in host defence against influenza virus infection. Biomed. J. 41 (4), 218–233. https://doi.org/10.1016/j.bj.2018.08.004.

Dobrescu, I., Levast, B., Lai, K., Delgado-Ortega, M., Walker, S., Banman, S., Townsend, H., Simon, G., Zhou, Y., Gerdts, V., Meurens, F., 2014. In vitro and ex vivo analyses of co-infections with swine influenza and porcine reproductive and respiratory syndrome viruses. Vet. Microbiol. 169 (1-2), 18–32. https://doi.org/10.1016/j.vetmic.2013.11.037.

Drappier, M., Michiels, T., 2015. Inhibition of the OAS/RNase L pathway by viruses. Curr. Opin. Virol. 15, 19–26. https://doi.org/10.1016/j.coviro.2015.07.002.

Dreiding, P., Staeheli, P., Haller, O., 1985. Interferon-induced protein Mx accumulates in nuclei of mouse cells expressing resistance to influenza viruses. Virology 140 (1), 192–196.

Frydas, I.S., Nauwynck, H.J., 2016. Replication characteristics of eight virulent and two attenuated genotype 1 and 2 porcine reproductive and respiratory syndrome virus (PRRSV) strains in nasal mucosa explants. Vet. Microbiol. 182, 156–162. https://doi.org/10.1016/j.vetmic.2015.11.016.

Glorieux, S., Bachert, C., Favoreel, H.W., Vandekerckhove, A.P., Steukers, L., Rekecki, A., Van den Broeck, W., Goossens, J., Croubels, S., Clayton, R.F., Nauwynck, H.J., Geraghty, R.J., 2011. Herpes simplex virus type 1 penetrates the basement membrane in human nasal respiratory mucosa. PLoS ONE 6 (7), e22160. https://doi.org/10.1371/journal.pone.0022160.

Glorieux, S., Favoreel, H.W., Meesen, G., de vos, W., Van den Broeck, W., Nauwynck, H.J., 2009. Different replication characteristics of historical pseudorabies virus strains in porcine respiratory nasal mucosa explants. Vet. Microbiol. 136 (3-4), 341–346. https://doi.org/10.1016/j.vetmic.2008.11.005.

Glorieux, S., Van den Broeck, W., van der Meulen, K.M., Van Reeth, K., Favoreel, H.W., Nauwynck, H.J., 2007. In vitro culture of porcine respiratory nasal mucosa explants for studying the interaction of porcine viruses with the respiratory tract. J. Virol. Methods 142 (1-2), 105–112. https://doi.org/10.1016/j.jviromet.2007.01.018.

Iwatsuki-Horimoto, K., Nakajima, N., Shibata, M., Takahashi, K., Sato, Y., Kiso, M., Yamayoshi, S., Ito, M., Enya, S., Otake, M., Kangawa, A., da Silva Lopes, T.J., Ito, H., Hasegawa, H., Kawaoka, Y., Schultz-Cherry, S., 2017. The microminipig as an animal model for influenza A virus infection. J. Virol. 91 (2) https://doi.org/10.1128/JVI.01716-16.

Jahnsen, F.L., Gran, E., Haye, R., Brandtzaeg, P., 2004. Human nasal mucosa contains antigen-presenting cells of strikingly different functional phenotypes. Am. J. Respir. Cell Mol. Biol. 30 (1), 31–37. https://doi.org/10.1165/rcmb.2002-0230OC.

Jang, Y.J., Lee, S.H., Kwon, H.-J., Chung, Y.-S., Lee, B.-J., 2005. Development of rhinovirus study model using organ culture of turbinate mucosa. J. Virol. Methods 125 (1), 41–47. https://doi.org/10.1016/j.jviromet.2004.12.004.

Jewell, N.A., Cline, T., Mertz, S.E., Smirnov, S.V., Flaño, E., Schindler, C., Grieves, J.L., Durbin, R.K., Kotenko, S.V., Durbin, J.E., 2010. Lambda interferon is the predominant interferon induced by influenza A virus infection in vivo. J. Virol. 84 (21), 11515–11522. https://doi.org/10.1128/JVI.01703-09.

Kato, H., Takeuchi, O., Sato, S., Yoneyama, M., Yamamoto, M., Matsui, K., Uematsu, S., Jung, A., Kawai, T., Ishii, K.J., Yamaguchi, O., Otsu, K., Tsujimura, T., Koh, C.-S., Reis e Sousa, C., Matsuura, Y., Fujita, T., Akira, S., 2006. Differential roles of MDA5 and RIG-I helicases in the recognition of RNA viruses. Nature 441 (7089), 101–105. https://doi.org/10.1038/nature04734.

Kim, S., Kim, M.-J., Park, D.Y., Chung, H.J., Kim, C.-H., Yoon, J.-H., Kim, H.J., 2015. Mitochondrial reactive oxygen species modulate innate immune response to influenza A virus in human nasal epithelium. Antiviral Res. 119, 78–83. https://doi.org/10.1016/j.antiviral.2015.04.011.

Klinkhammer, J., Schnepf, D., Ye, L., Schwaderlapp, M., Gad, H.H., Hartmann, R., Garcin, D., Mahlakõiv, T., Staeheli, P., 2018. IFN-λ prevents influenza virus spread from the upper airways to the lungs and limits virus transmission. Elife 7. https://doi.org/10.7554/eLife.33354.

Knight, D.A., Holgate, S.T., 2003. The airway epithelium: Structural and functional properties in health and disease. Respirology 8 (4), 432–446. https://doi.org/10.1046/j.1440-1843.2003.00493.x.

Mazzetto, E., Bortolami, A., Fusaro, A., Mazzacan, E., Maniero, S., Vascellari, M., Beato, M.S., Schiavon, E., Chiapponi, C., Terregino, C., Monne, I., Bonfante, F., 2020. Replication of influenza D viruses of bovine and swine origin in ovine respiratory explants and their attachment to the respiratory tract of bovine, sheep, goat, horse, and swine. Front. Microbiol. 11 https://doi.org/10.3389/fmicb.2020.01136.

Min, J.-Y., Krug, R.M., 2006. The primary function of RNA binding by the influenza A virus NS1 protein in infected cells: Inhibiting the 2'-5' oligo (A) synthetase/RNase L pathway. Proc. Natl. Acad. Sci. 103 (18), 7100–7105. https://doi.org/10.1073/pnas.0602184103.

Nagy, A., Vostinakova, V., Pirchanova, Z., Cernikova, L., Dirbakova, Z., Mojzis, M., Jirincova, H., Havlickova, M., Dan, A., Ursu, K., Vilcek, S., Hornickova, J., 2010. Development and evaluation of a one-step real-time RT-PCR assay for universal detection of influenza A viruses from avian and mammal species. Arch. Virol. 155 (5), 665–673. https://doi.org/10.1007/s00705-010-0636-x.

Niesalla, H.S., Dale, A., Slater, J.D., Scholes, S.F.E., Archer, J., Maskell, D.J., Tucker, A. W., 2009. Critical assessment of an in vitro bovine respiratory organ culture system: A model of bovine herpesvirus-1 infection. J. Virol. Methods 158 (1-2), 123–129. https://doi.org/10.1016/j.jviromet.2009.02.001.

Nonnemann, B., Lyhs, U., Svennesen, L., Kristensen, K.A., Klaas, I.C., Pedersen, K., 2019. Bovine mastitis bacteria resolved by MALDI-TOF mass spectrometry. J. Dairy Sci. 102 (3), 2515–2524. https://doi.org/10.3168/jds.2018-15424.

Palm, M., Garigliany, M.-M., Cornet, F., Desmecht, D., 2010. Interferon-induced Sus scrofa Mx1 blocks endocytic traffic of incoming influenza A virus particles. Vet. Res. 41 (3), 29. https://doi.org/10.1051/vetres/2010001.

Pena, L., Vincent, A.L., Loving, C.L., Henningson, J.N., Lager, K.M., Lorusso, A., Perez, D. R., 2012. Restored PB1-F2 in the 2009 pandemic H1N1 influenza virus has minimal effects in swine. J. Virol. 86 (10), 5523–5532.

Pichlmair, A., Schulz, O., Tan, C.P., Näslund, T.I., Liljeström, P., Weber, F., Reis e Sousa, C., 2006. RIG-I-mediated antiviral responses to single-stranded RNA bearing 5′-phosphates. Science 314 (5801), 997–1001.

Pol, J.M.A., Quint, W.G.V., Kok, G.L., Broekhuysen-Davies, J.M., 1991. Pseudorabies virus infections in explants of porcine nasal mucosa. Res. Vet. Sci. 50 (1), 45–53. https://doi.org/10.1016/0034-5288(91)90052-P.

Rajao, D.S., Vincent, A.L., 2015. Swine as a model for influenza A virus infection and immunity. ILAR J. 56 (1), 44–52. https://doi.org/10.1093/ilar/ilv002.

Reed, L.J., Muench, H., 1938. A simple method of estimating fifty per cent endpoints. Am. J. Epidemiol. 27, 493–497. https://doi.org/10.1093/oxfordjournals.aje.a118408.

Roberts, K.L., Shelton, H., Scull, M., Pickles, R., Barclay, W.S., 2011. Lack of transmission of a human influenza virus with avian receptor specificity between ferrets is not due to decreased virus shedding but rather a lower infectivity in vivo. J. Gen. Virol. 92, 1822–1831. https://doi.org/10.1099/vir.0.031203-0.

Shinya, K., Ebina, M., Yamada, S., Ono, M., Kasai, N., Kawaoka, Y., 2006. Influenza virus receptors in the human airway. Nature 440 (7083), 435–436. https://doi.org/10.1038/440435a.

Skovgaard, K., Cirera, S., Vasby, D., Podolska, A., Breum, S.Ø., Dürrwald, R., Schlegel, M., Heegaard, P.MH., 2013. Expression of innate immune genes, proteins and microRNAs in lung tissue of pigs infected experimentally with influenza virus (H1N2). Innate Immun. 19 (5), 531–544. https://doi.org/10.1177/1753425912473668.

Spicer, S.S., Schulte, B.A., Thomopoulos, G.N., 1983. Histochemical properties of the respiratory tract epithelium in different species. Am. Rev. Respir. Dis. 128, 20–26. https://doi.org/10.1164/arrd.1983.128.2P2.S20.

Starbæk, S.M.R., Brogaard, L., Dawson, H.D., Smith, A.D., Heegaard, P.M.H., Larsen, L.E., Jungersen, G., Skovgaard, K., 2018. Animal models for Influenza A virus infection incorporating the involvement of innate host defenses: enhanced translational value of the porcine model. ILAR J. 59 (3), 323–337. https://doi.org/10.1093/ilar/ily009.

Steukers, L., Vandekerckhove, A.P., Broeck, W. Van Den, Glorieux, S., Nauwynck, H.J., (2012). Kinetics of BoHV-1 dissemination in an in vitro culture of bovine upper respiratory tract mucosa explants. ILAR J. 53, 43–54. doi:10.1093/ilar.53.1.43.

Tan, K.S., Yan, Y., Koh, W.L.H., Li, L., Choi, H., Tran, T., Sugrue, R., Wang, D.Y., Chow, V.T., 2018. Comparative transcriptomic and metagenomic analyses of influenza virus-infected nasal epithelial cells from multiple individuals reveal specific nasal-initiated signatures. Front. Microbiol. 9 https://doi.org/10.3389/fmicb.2018.02685.

Tannenbaum, J., Bennett, B.T., 2015. Russell and Burch's 3Rs then and now: The need for clarity in definition and purpose. J. Am. Assoc. Lab. Anim. Sci. 54, 120–132.

Trebbien, R., Larsen, L.E., Viuff, B.M., 2011. Distribution of sialic acid receptors and influenza A virus of avian and swine origin in experimentally infected pigs. Virol. J. 8, 434. https://doi.org/10.1186/1743-422X-8-434.

Tulinski, P., Fluit, A.C., van Putten, J.P.M., de Bruin, A., Glorieux, S., Wagenaar, J.A., Duim, B., Smith, T.C., 2013. An ex vivo porcine nasal mucosa explants model to study MRSA colonization. PLoS ONE 8 (1), e53783. https://doi.org/10.1371/journal.pone.0053783.

Vairo, S., Van Den Broeck, W., Favoreel, H., Scagliarini, A., Nauwynck, H., 2013. Development and use of a polarized equine upper respiratory tract mucosal explant system to study the early phase of pathogenesis of a European strain of equine arteritis virus. Vet. Res. 44, 1–9. https://doi.org/10.1186/1297-9716-44-22.

Van Poucke, S., Uhlendorff, J., Wang, Z., Billiau, V., Nicholls, J., Matrosovich, M., Van Reeth, K., 2013. Effect of receptor specificity of A/Hong Kong/1/68 (H3N2) influenza virus variants on replication and transmission in pigs. Influenza Other Respi. Viruses 7 (2), 151–159. https://doi.org/10.1111/j.1750-2659.2012.00376.x.

Van Poucke, S.G., Nicholls, J.M., Nauwynck, H.J., Van Reeth, K., 2010. Replication of avian, human and swine influenza viruses in porcine respiratory explants and association with sialic acid distribution. Virol. J. 7, 1–14. https://doi.org/10.1186/1743-422X-7-38.

Vandesompele, J., De Preter, K., Pattyn, F., Poppe, B., Van Roy, N., De Paepe, A., et al., (2002). Accurate normalization of real-time quantitative RT-PCR data by geometric averaging of multiple internal control genes. Genome Biol. 3, research0034.1–0034.11. doi:10.1613/jair.4265.

Verhelst, J., Parthoens, E., Schepens, B., Fiers, W., Saelens, X., 2012. Interferon-inducible protein Mx1 inhibits influenza virus by interfering with functional viral ribonucleoprotein complex assembly. J. Virol. 86 (24), 13445–13455.

Wallace, P., Kennedy, J.R., Mendicino, J., 1994. Transdifferentiation of outgrowth cells and cultured epithelial cells from swine trachea. Vitr. Cell. Dev. Biol. - Anim. 30 (3), 168–180. https://doi.org/10.1007/BF02631440.

Webster, R.G., Bean, W.J., Gorman, O.T., Chambers, T.M., Kawaoka, Y., 1992. Evolution and ecology of influenza A viruses. Microbiol. Rev. 56 (1), 152–179. https://doi.org/10.1128/mr.56.1.152-179.1992.

Yan, Y., Tan, K.S., Li, C., Tran, T., Chao, S.S., Sugrue, R.J., et al., 2016. Human nasal epithelial cells derived from multiple subjects exhibit differential responses to H3N2 influenza virus infection in vitro. J. Allergy Clin. Immunol. 138, 276–281.e15. https://doi.org/10.1016/j.jaci.2015.11.016.

Yoon, S.-W., Webby, R.J., Webster, R.G., (2014). Evolution and Ecology of Influenza A Viruses. In: Current Topics in Microbiology and Immunology. pp. 359–375. doi:10.1007/82_2014_396.

Zhang, L., Button, B., Gabriel, S.E., Burkett, S., Yan, Y.u., Skiadopoulos, M.H., Dang, Y.L., Vogel, L.N., McKay, T., Mengos, A., Boucher, R.C., Collins, P.L., Pickles, R.J., Philipson, L., 2009. CFTR delivery to 25% of surface epithelial cells restores normal rates of mucus transport to human cystic fibrosis airway epithelium. PLoS Biol. 7 (7), e1000155. https://doi.org/10.1371/journal.pbio.1000155.